Available online at www.sciencedirect.com

ScienceDirect

Procedia Structural Integrity 62 (2024) 323–330

Structural Integrity Procedia

www.elsevier.com/locate/procedia

II Fabre Conference – Existing bridges, viaducts and tunnels: research, innovation and applications (FABRE24)

Influence of chloride-induced corrosion on the traffic vulnerability of simply supported Italian PC bridges: a preliminary study

Stefano Bozza[a,*], Marco Fasan[a], Chiara Bedon[a], Salvatore Noè[a]

[a]*Università degli studi di Trieste, Dipartimento di Ingegneria e Architettura, via A. Valerio 6, Trieste 34127, Italy*

Abstract

In Italy, a large part of road bridges was built after the Second World War, mainly with Reinforced Concrete (RC) or Prestressed Concrete (PC) simply supported decks. Most of the bridges currently in service have been designed with outdated codes and could be inadequate to modern heavy traffic loads. Furthermore, their structural performance decrease over time due to ageing effects, like steel corrosion.

Bridges are often exposed to chlorides from de-icing salts or marine environment; chloride diffusion in concrete can induce pitting corrosion of steel reinforcing, decreasing the structural resistance of bridge elements. As part of a broader study on the structural risk of existing bridges with respect to traffic loads, it is certainly of interest to investigate the influence of chloride-induced corrosion on the risk itself.

In this preliminary study, four sets of simply supported decks made of precast PC beams and a cast in-situ RC slab were designed according to outdated Italian codes relating to different construction periods (60s, 70s, 80s, and 90s); each set is composed by bridges with different span, width, number of main girders and transverse diaphragms. The deck design took into account only the bending failure of the main girders, in order to determine the minimum amount of strands and steel reinforcements required. The vulnerability to traffic loads is evaluated with respect to the bending moment resistance of the main girders. Monte Carlo simulations were performed to evaluate the decrease over time of the resisting bending moment of the main girders, taking into account literature models for estimating the time to corrosion and corrosion propagation both in strands and in steel reinforcements.

* Corresponding author.
E-mail address: stefano.bozza@phd.units.it

2452-3216
10.1016/j.prostr.2024.09.048

Keywords: Traffic vulnerability; corrosion; existing PC bridges; Monte Carlo simulations.

1. Introduction

Bridges are critical elements of road networks, and they can be subjected to both natural hazards (Argyroudis and Mitoulis (2021)) and man-made hazards, e.g. overloading (Yan et al. (2019)). Furthermore, structural performance of bridges decrease over time due to ageing effects, such as chloride-induced corrosion.

In Italy, a large part of the road bridges was built after the Second World War, mainly with Reinforced Concrete (RC) or Prestressed Concrete (PC) simply supported decks (Pinto and Franchin (2010), Borzi et al. (2015)), in according to outdated codes.

Over the last century, both traffic load models and technical requirements have undergone a continuous evolution; whilst the evolution of the traffic load models for road bridges has been investigate (Bozza et al. (2023)), the influence of the evolution of the technical codes has not.

Moreover, existing bridges could be exposed to chloride environment: chloride ions penetration can induce pitting corrosion, decreasing the resistance of the main structural members over time.

In this preliminary study, four sets of simply supported decks made of precast PC beams and a cast in-situ RC slab were designed according to Italian outdated codes relating to different construction periods (60s, 70s, 80s, and 90s); bridges with different span, width, number of main girders and transverse diaphragms, compose each set. The deck design took into account only the bending failure of the main girders, in order to determine the minimum amount of strands and steel reinforcements required.

The vulnerability to traffic load is evaluated with respect to the bending moment resistance of the main girders, by means of fragility curves as proposed by Miluccio et al. (2021). Monte Carlo simulations were performed to evaluate the decrease over time of the resisting bending moment of the main girders, taking into account literature models for estimating the time to corrosion and corrosion propagation both in prestressing strands and in steel reinforcements.

2. Bridge deck design according to outdated code evolution

2.1. Traffic load models evolution

The evolution of the Italian codes on traffic loads have been investigated in previous study (Bencivenga et al. (2022), Bozza et al. (2023)), so it is not reported for sake of brevity. For the construction periods taken into account in the present paper, were considered the following regulations:

- Circular no. 384 of February 14th, 1962 for both 60s and 70s bridges;
- Ministry Decree no. 308 of August 2nd, 1980 for 80s bridges;
- Ministry Decree of May 4th, 1990 for 90s bridges.

2.2. Technical codes evolution

The evolution of the Italian technical codes with respect to RC elements started mode than a century ago, with the Ministry Decree of January 10th, 1907. Prestressed elements were taken into account in the regulations only after the Second World War, starting with the Decree of the Provisional Head of State December 2nd, 1947, and some subsequent Circulars of the High Council of Public Works. From 1972 onwards, PC standards were present in the main technical code for RC, PC and steel construction, which was updated several times over the years. For the construction periods taken into account in the present paper, were considered the following regulations:

- Circular no. 494 of March 7th, 1960 for 60s bridges;
- Ministry Decree of May 30nd, 1972 for 70s bridges;
- Ministry Decree of July 27nd, 1985 for 80s bridges;
- Ministry Decree of February 14th, 1992 for 90s bridges.

2.3. Deck design

For each construction period considered, a sample of simply supported PC girder bridges was designed against flexural failure of the main girders, in order to determine the minimum amount of reinforcement bars and prestressing strands required. Initially, a set of deck geometries was defined considering spans ranging from 10 m to 40 m (discretized every 5 m), widths ranging from 8 m to 16 m (discretized every 2 m), and lateral kerb width equal to 0.5 m or 1.0 m. For every span, two to four number of transverse diaphragms were considered, with spacing varying from a minimum of 5 m and a maximum of 15 m, while for every width, four number of longitudinal PC beams were considered, with beam spacing between 1.0 m and 3.0 m. The slab thickness was assumed equal to 0.20 m, while the transverse diaphragms thickness was assumed equal to 0.30 m. The sections of the precast PC beams were selected from a database of precast PC sections in order to obtain a beam height over span ratio as close as possible to 1/18 and the height of the transverse diaphragms was assumed equal to the height of the longitudinal beam minus the height of the bottom flange of the beam. For each geometry, the maximum bending moment due to dead loads and outdated traffic load models were evaluated via the Guyon – Massonnnet – Bareš method (Bareš and Massonnet (1957)).

An ordinary concrete ($f_{ck} = 25$ MPa) was assumed for the cast in-situ slab, while a good concrete ($f_{ck} = 40$ MPa) was assumed for the precast PC beams. Mild steel for rebars was assumed as a medium quality steel, according to outdated regulations, while prestressing strand steel was assumed with $f_{p,01}$ equal to 1600 MPa, according to historical technical documentation. The probability distribution of the materials properties are reported in Table 1.

The number of reinforced bars was fixed to 8Φ10 bars both in the bottom flange and in the top flange, considering a cover equal to 20 mm. The number of prestressing strands was designed in order to verify the flexural failure check according to outdated regulations; both 0.5’ and 0.6’ strands were considered, with spacing respectively of 0.04 m and 0.05 m. The strands were positioned only in the bottom flange; if the maximum number of strands that fit in the bottom flange was not enough to verify the flexural failure check, the geometry was discarded.

Table 1. Probabilistic variables for materials properties.

Variable	Units	Distribution	μ	σ	Note
Slab concrete compression strength f_c	MPa	Lognormal	33.0	5.28	$f_{cm} = f_{ck} + 8$ MPa (NTC (2018))
Precast beam concrete compression strength f_c	MPa	Lognormal	48.0	4.80	$f_{cm} = f_{ck} + 8$ MPa (NTC (2018))
Aq50 yield stress f_y (60s bridges)	MPa	Lognormal	369.9	29.4	Verderame et al. (2000)
FeB38k yield stress f_y (70s, 80s, 90s bridges)	MPa	Lognormal	469.0	37.5	CoV similar to Verderame et al. (2000)
Strands conventional yield stress $f_{p,01}$	MPa	Lognormal	1643	26.3	

3. Chloride-induced corrosion

Road bridges can be exposed to chloride environment, as in marine-prone zone or due to de-icing salts; studies have observed that pitting corrosion rather than uniform corrosion is the primary deterioration form (Cui et al. (2018)). In this preliminary study, the pitting corrosion over time is modelled as suggested in Tuutti (1982), with an initiation phase related to the penetration of chloride ions towards the concrete cover and a propagations phase, with a progressive loss of steel due to corrosion.

The time to corrosion t_i is evaluated according to DuraCrete (2000):

$$t_i = X_I \left\{ \frac{{d_c}^2}{4\, k_e\, k_t\, k_c\, D_0\, {t_0}^n} \left[erf^{-1}\left(1 - \frac{C_{cr}}{C_S}\right)\right]^{-2} \right\}^{\frac{1}{1-n}} \quad (1)$$

In which X_I is the model uncertainty coefficient, d_c is the concrete cover, k_e is the environmental factor, k_t is the test method factor, k_t is the curing time correction factor, D_0 is the diffusion factor at reference period, t_0 is the reference period (28 days), n is the aging factor, C_{cr} is the critical value of the chloride ion concentration, and C_S is the chloride ion concentration on the concrete surface, modelled as:

$$C_S = A_{CS}\,(w/c) + \varepsilon_{CS} \tag{2}$$

Where w/c is the water-to-binder ratio, A_{CS} and ε_{CS} are model parameters.
In the present study, the parameters were assumed as reported in Table 2.

Table 2. Probabilistic variables for corrosion initiation.

Variable	Units	Distribution	μ	σ	a	b	Note
Model uncertainty X_I	-	Normal	1.00	0.05	-	-	DuraCrete (2000)
Environmental correction factor k_e	-	Gamma	0.676	0.114	-	-	Duracrete (2000)
Correction factor for tests k_t	-	Normal	0.832	0.024	-	-	DuraCrete (2000)
Curing time correction factor k_c	-	Deterministic	1.00	-	-	-	DuraCrete (2000)
Reference diffusion coefficient D_0	m^2/s	Normal	$8.9 \cdot 10^{-12}$	$1.78 \cdot 10^{-12}$	-	-	Fib (2006)
Reference time t_0	yr	Deterministic	0.0767	-	-	-	DuraCrete (2000)
Critical chloride content C_{cr}	mass - %/cement	Beta	0.60	0.15	0.2	2.0	Fib (2006)
Chloride surface content - A_{CS}	mass - %/cement	Normal	2.656	0.356	-	-	DuraCrete (2000)
Chloride surface content- ε_{CS}	mass - %/cement	Normal	0.00	0.405	-	-	DuraCrete (2000)
Ageing exponent n	-	Beta	0.30	0.12	0.0	1.0	Fib (2006)

After the chloride-induced corrosion initiation, reinforcement bars and strands decrease their section due to the formation of pits; usually, the pit geometry is assumed as hemispherical, as proposed by Val and Melchers (1997), so that the residual area of a circular section can be calculated as:

$$A(t) = \begin{cases} A_0 - A_1(t) - A_2(t) & if\ p(t) \le \frac{\sqrt{2}\,d_b}{2} \\ A_1(t) - A_2(t) & if\ \frac{\sqrt{2}\,d_b}{2} \le p(t) \le d_b \\ 0 & if\ p(t) \ge d_b \end{cases} \tag{3}$$

$$A_0 = \frac{\pi\,{d_b}^2}{4}\ ;\ A_1(t) = \frac{1}{2}\left[\theta_1(t)\left(\frac{d_b}{2}\right)^2 - a(t)\left|\frac{d_b}{2} - \frac{p(t)^2}{d_b}\right|\right]\ ;\ A_2(t) = \frac{1}{2}\left[\theta_2(t)\,p(t)^2 - a(t)\frac{p(t)^2}{d_b}\right] \tag{4}$$

$$a(t) = 2\,p(t)\sqrt{1 - \left[\frac{p(t)}{d_b}\right]^2}\ ;\ \theta_1(t) = 2\,sin^{-1}\left(\frac{2a(t)}{d_b}\right)\ ;\ \theta_2(t) = 2\,sin^{-1}\left(\frac{a(t)}{p(t)}\right) \tag{5}$$

Where $p(t)$ is the pit depth at time t, d_b is the diameter of the bar, $a(t)$, $\theta_1(t)$, and $\theta_2(t)$ are pit parameters depending on $p(t)$ and d_b.
The corrosion rate was modelled following Vu and Stewart (2000):

$$i_{corr}(t) = i_{corr}(1) \cdot 0.85\,(t - t_i)^{-0.29} \tag{6}$$

$$i_{corr}(1) = \frac{37.8\cdot(1-w/c)^{-1.64}}{d_c} \tag{7}$$

Where $i_{corr}(t)$ is the corrosion rate at time t, and $i_{corr}(1)$ is the corrosion rate at the start of corrosion propagation, both expressed in $\mu A/cm^2$ given the cover in mm.
The maximum pit depth in the reinforcement bars was calculated:

$$p(t) = 0.0116 \cdot R \cdot \int_{t_i}^{t} i_{corr}(\tau)\,d\tau \tag{8}$$

In which R is the pitting factor, calculated as proposed by Pugliese and Di Sarno (2022).

The maximum pit depth in the strand wires was calculated using the probability distribution proposed in Darmawan and Stewart (2007):

$$f_p(t, i_{corr},\ L) = \frac{\alpha}{\lambda(t)^{0.54}} e^{-\alpha\left(\frac{p}{\lambda(t)^{0.54}}\mu\right)} e^{-e^{-\alpha\left(\frac{p}{\lambda(t)^{0.54}}\mu\right)}} \tag{9}$$

$$\lambda = \frac{\left[{d_w}^2 - \left(d_w - 0.0232\, i_{corr}(1)\left\{1+\frac{\kappa}{\theta+1}\left[(t-t_i)^{\theta+1}-1\right]\right\}\right)^2\right]}{\left[{d_w}^2 - \left(d_w - 0.0232\, i_{corr}(1)\left\{1+\frac{\kappa}{\theta+1}\left[{t_0}^{\theta+1}-1\right]\right\}\right)^2\right]} \tag{10}$$

$$t_0 = exp\left[\frac{\kappa}{\theta+1}\ ln\left(\frac{(\theta+1)\left(i_{corr,exp}\, t_{exp}\right) + (\kappa-\theta-1)\, i_{corr}(1)}{\kappa\, i_{corr}(1)}\right)\right]\ ;\ \mu = \mu_{exp} + \frac{1}{\alpha_{exp}} ln\left(\frac{L}{L_{exp}}\right)\ ;\ \alpha = \alpha_{exp} \tag{11}$$

In which d_w is the diameter of the wire, α_{exp}, μ_{exp}, L_{exp}, $i_{corr,exp}$, and t_{exp} are experimental parameters (respectively equal to 8.10, 0.84, 650 mm, 186 μA/cm^2, and 0.03836 years), κ and θ are corrosion rate empirical factors (respectively 0.89 and –0.29, according to (6)), and L is the wire length. In this study, the capacity was evaluated for the midspan section, and a length equal to 1 m was considered.

In the present study, the parameters of the corrosion propagation were assumed as reported in Table 3.

Table 3. Probabilistic variables for corrosion propagation.

Variable	Units	Distribution	μ	σ	k	Note
Model uncertainty for i_{corr} (Eq. (6))	-	Uniform	1.00	0.20	-	Vu and Stewart (2000)
Pitting factor in reinforcement bars R	-	GEV	3.82	1.28	0.01	Pugliese and Di Sarno (2022)
Pit depth in strand wires f_p	mm	Gumbel	Eq. (9), (10), (11)			Darmawan and Stewart (2007)

4. Methodology

The vulnerability to traffic loads is evaluated by means of fragility curves as proposed by Miluccio et al. (2021), considering the traffic load multiplier α as Intensity Measure (IM). The structural analyses of each deck of the four sets of bridges were carried out via the Guyon – Massonnet – Bareš method, in order to estimate the maximum bending moment of the main girders due to structural permanent loads (g_1), non-structural permanent loads (g_2) and traffic loads (q) (calculated according to the current Italian regulations, NTC(2018)). To consider the variability of dead loads, a sample of 10^3 values of g_1 and g_2 was generated for every deck, following a normal distribution with CoV respectively equal to 0.05 and 0.10, as Miluccio et al. (2021), whilst the variability of the maximum bending moment induced by traffic loads is neglected.

The capacity (ultimate bending strength), of the main girders were evaluated following the assumption of plane cross-section, perfect concrete-steel bonding, parabola-rectangle stress diagram for concrete under compression, with ultimate strain equal to 0.35%, elastic-perfectly plastic behaviour for mild and prestressing steel. The "as-built" capacity, calculated without the effects of corrosion, is evaluated on a 10^3 sample of the material random variables (as reported in Table 1) for each deck of each set. The "today" capacity is evaluated also accounting for a 10^3 sample of corrosion random variables (as reported in Table 2 and Table 3), calculated considering the time since construction, approximated to 60 years, 50 years, 40 years, and 30 years for 60s, 70s, 80s, and 90s bridges respectively.

In the present study, the fragility to traffic loads is the probability to have a demand bending moment equal or higher than the ultimate bending moment (M_R) given a load multiplier α:

$$P[failure\ |\alpha\ ] = P\left[\left(M_{g1} + M_{g2} + \alpha\ M_q\right)\ \geq M_R\ \middle|\ \alpha\ \right] \tag{12}$$

The failure condition can be re-written as:

$$P[failure\ |\alpha\ ] = P\left[\frac{M_R - M_{g1} - M_{g2}}{M_q} \leq \alpha \mid \alpha\right] = CDF\left(\frac{M_R - M_{g1} - M_{g2}}{M_q}\right) \quad (13)$$

The fragility curves were derived by fitting a lognormal distribution to the ratio $\left[\left(\mathrm{M_R} - \mathrm{M_{g1}} - \mathrm{M_{g2}}\right)/\mathrm{M_q}\right]$ via the maximum likelihood method, minimizing the negative log-likelihood.

5. Results

The fragility curves for first class bridges and second class bridges for each construction period were calculated as previously described. Since the span of the deck influences the vulnerability to traffic loads (Bozza et al. (2023)), the fragility curves were evaluate for each span considered in this study. The parameters of the fragility curves are reported in Table 4, whilst fragility curves are graphically reported in Figure 1.

Table 4. Parameters of the fragility curves (mean and standard deviation of the lognormal distribution).

		60s				70s				80s				90s			
		1° class		2° class		1° class		2° class		1° class		2° class		1° class		2° class	
Span	Moment	μ	σ	μ	σ	μ	σ	μ	σ	μ	σ	μ	σ	μ	σ	μ	σ
10 m	as-built	2.10	0.13	1.46	0.15	1.87	0.13	1.30	0.13	2.03	0.11	1.40	0.10	2.23	0.11	2.00	0.13
	today	1.54	0.37	0.99	0.32	1.40	0.31	0.94	0.26	1.64	0.29	1.11	0.23	2.08	0.27	1.71	0.25
15 m	as-built	2.20	0.11	1.50	0.14	1.97	0.11	1.33	0.14	2.14	0.13	1.46	0.11	2.29	0.11	1.96	0.13
	today	1.66	0.36	1.08	0.32	1.55	0.29	1.00	0.27	1.77	0.28	1.17	0.24	2.04	0.26	1.71	0.23
20 m	as-built	2.40	0.19	1.81	0.19	2.14	0.17	1.61	0.17	2.28	0.18	1.63	0.16	2.36	0.15	2.05	0.17
	today	1.89	0.37	1.36	0.59	1.70	0.34	1.26	0.65	1.92	0.29	1.32	0.44	2.10	0.25	1.78	0.25
25 m	as-built	2.57	0.21	2.04	0.21	2.28	0.19	1.81	0.19	2.43	0.18	1.74	0.17	2.45	0.16	2.14	0.19
	today	2.07	0.36	1.57	0.43	1.86	0.32	1.42	0.44	2.10	0.28	1.42	0.39	2.23	0.25	1.90	0.24
30 m	as-built	2.98	0.26	2.42	0.27	2.61	0.24	2.12	0.24	2.69	0.22	2.02	0.21	2.63	0.19	2.37	0.24
	today	2.39	0.45	1.89	0.49	2.13	0.38	1.68	0.49	2.30	0.33	1.66	0.41	2.43	0.30	2.09	0.29
35 m	as-built	3.56	0.36	2.90	0.38	3.06	0.31	2.52	0.32	3.01	0.26	2.36	0.29	2.87	0.24	2.69	0.31
	today	2.78	0.61	2.24	0.70	2.46	0.49	1.99	0.67	2.52	0.42	1.93	0.56	2.72	0.38	2.34	0.37
40 m	as-built	3.86	0.36	3.07	0.39	3.29	0.31	2.63	0.34	3.09	0.26	2.42	0.30	2.92	0.23	2.76	0.31
	today	3.03	0.64	2.38	0.56	2.66	0.50	2.09	0.49	2.61	0.42	2.00	0.40	2.85	0.38	2.43	0.37

As expected, second class bridges are more fragile than first class bridges, and short bridges are more fragile than longer bridges, according to previous study (Bozza et al. (2023)). Considering the “as-built” configuration, first class 60s bridges are the less vulnerable ones, with the exception of bridges shorter than 20 m, which have an higher vulnerability than 90s first class bridges: this indicates that Circular no. 494 of 1960 is very conservative. For first class bridges with span higher than 30 m, 90s bridge are the most vulnerable, while for shorter span 70s bridges are the most vulnerable. For second class bridges, 70s short bridges and 80s long bridges are the most vulnerable (both in the “as-built” configuration and considering the corrosion effects over time).

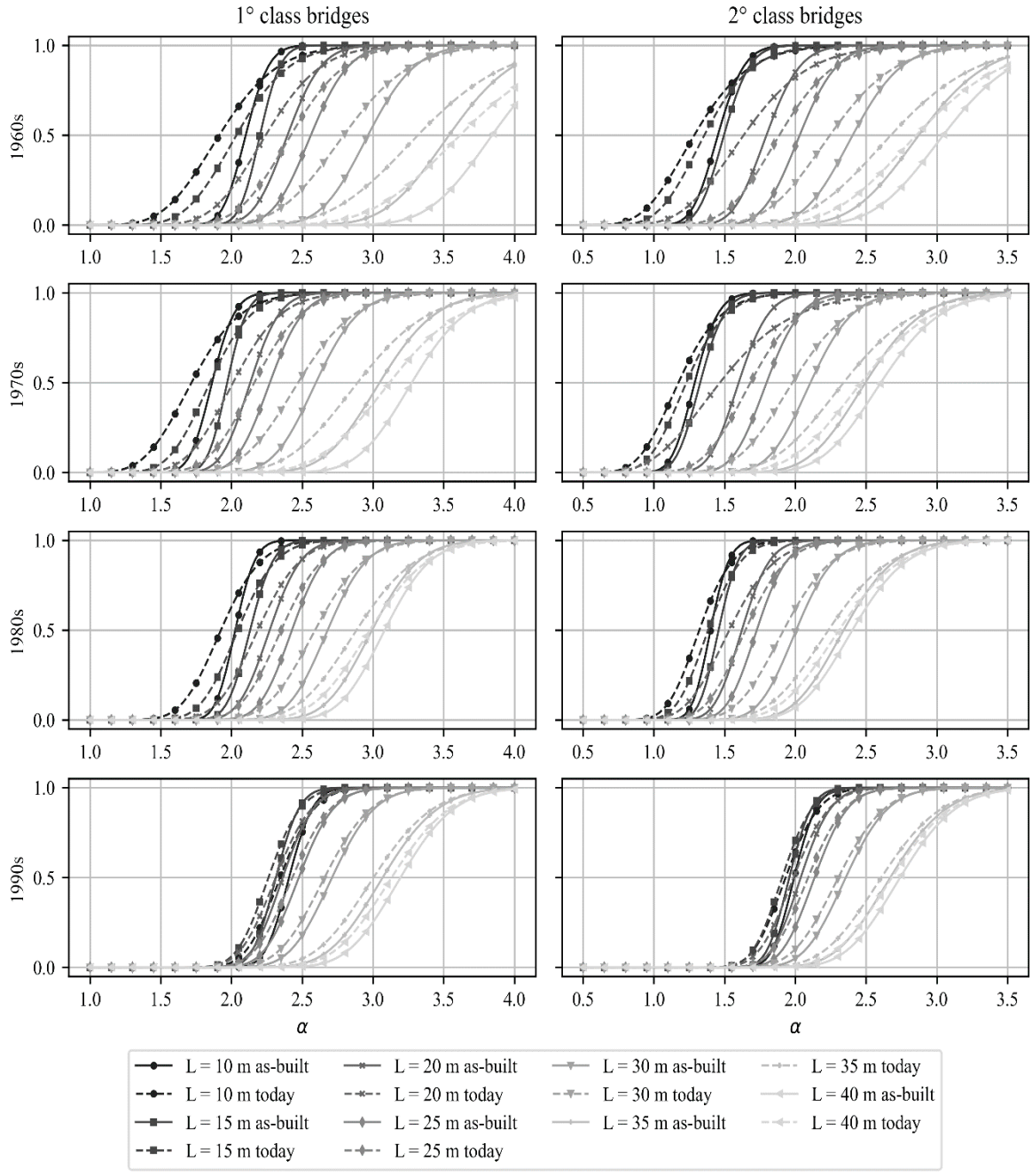

Figure 1. Fragility curves for different construction period, reference time and span for first class bridges and second class bridges.

Considering the effects of corrosion, 90s bridges are less vulnerable with respect to older ones, with the exception of first class bridges longer than 30 m, which are more vulnerable compared to 60s first class ones.

Generally, corrosion decrease the median and increase the dispersion of the fragility curves, with higher effects on second class bridges than on first class ones, and higher effects on short span bridges than on long span bridges. This seems to indicate that sections with less resistance are more sensitive to the effects of corrosion.

6. Conclusion

The vulnerability to traffic loads of typical existing Italian bridges has been investigated, focusing on simply supported PC girder bridges. The traffic vulnerability to traffic loads was evaluated for several bridges with different geometry, taking into account historical traffic load models, outdated technical codes, and different bridge classes. Ageing effects were also taken into account by means of a pitting corrosion model in both mild steel bars and prestressing strands. Fragility curves were derived for bridges with different span, period of construction, and bridge class, both in the "as-built" configuration (without corrosion) and accounting for pitting corrosion effects.

Acknowledgements

The authors would like to acknowledge Consorzio Fabre for providing financial support to part of research activities.

References

Argyroudis, S. A.; Mitoulis, S. A., 2021. Vulnerability of bridges to individual and multiple hazards - floods and earthquakes. Reliability Engineering & System Safety 210, 107564. https://doi.org/10.1016/j.ress.2021.107564

Bareš, R.; Massonnet, C. (1966). Les calcul des grillages de poutres et dalles orthotropes. Paris: Dunod.

Pinto, P. E.; Franchin, P. 2010. Issues in the Upgrade of Italian Highway Structures. Journal of Earthquake Engineering, 14, 1221-1252.

Borzi, B.; Ceresa, P.; Franchin, P.; Noto, F.; Calvi, G. M.; Pinto, P. E., 2015. Seismic vulnerability of the Italian roadway bridge stock. Earthquake Spectra 31, 4. https://doi.org/10.1193/070413EQS190M

Bozza, S., Fasan, M., Noè, S., 2023. Vulnerability to traffic loads of typical Italian bridges in relation to the evolution of the code framework. ce/papers, 6, 760-767. https://doi.org/10.1002/cepa.2038

Cui, F.; Zhang, H.; Ghosn, M.; Xu, Y., 2018. Seismic fragility analysis of deteriorating RC bridge substructures subject to marine chloride-induced corrosion. Engineering Structures 155, pp. 61-72. https://doi.org/10.1016/j.engstruct.2017.10.067

Darmawan M. S.; Stewart, M. G., 2007. Spatial time-dependent reliability analysis of corroding pretensioned prestressed concrete bridge girders. Structural Safety 29, pp. 16-31.

DuraCrete, 2000. Statistical quantification of the variables in the limit state functions. The European Union - Brite EuRam III.

Fib, 2006. Model Code for Service Life Design. Fib Bulletin 34.

Miluccio, G.; Losanno, D.; Parisi, F.; Cosenza, E., 2021. Traffic-load fragility models for prestressed concrete girder decks of existing Italian highway bridges. Engineering Structures 249, pp.113367

NTC (2018). Aggiornamento delle «Norme Tecniche per le Costruzioni» (in Italian).

Tuutti, K., 1982. Corrosion of steel in concrete. Doctoral Thesis, Division of Building Materials, Swedish Cement and Concrete Research Institute, Stockholm.

Val D. V., Melchers R. E., 1997. Reliability of deteriorating RC slab bridges. Journal of Structural Engineering 123 (12), pp.1638–1644.

Vu, K. A. T.; Stewart, M. G., 2000. Structural reliability of concrete bridges including improved chloride-induced corrosion models. Structural Safety 22, pp. 313-333.

Yan, W.; Deng, L.; Zhang, F.; Li, T.; Li, S., 2019. Probabilistic machine learning approach to bridge fatigue failure analysis due to vehicular overloading. Engineering Structures 193, p. 91–99. https://doi.org/10.1016/j.engstruct.2019.05.028